CHALMERS

Alpha wave recording using high-T_c SQUIDs

Master of Science Thesis

GERARD AMOROS FIGUERAS

Quantum Device Physics Laboratory
Department of Microtechnology and Nanoscience
CHALMERS UNIVERSITY OF TECHNOLOGY
Göteborg, Sweden, 2010

Abstract

This project aims to contribute to the creation of an MRI-MEG system to investigate and understand in a better way how the brain works. The main objective is to determine theoretically and empirically that high critical temperature SQUIDS are capable of measuring the strongest magnetic signals from human brain, named alpha waves.

A magnetometer built at Chalmers has been used to successfully record brain signals in a noise free environment with a resolution of 40 fT/√Hz at 10 Hz. This project is the "proof of principle" that these types of recordings are feasible and that can overcome the traditional MEG systems used nowadays in medicine. This study has to be expanded to fully confirm the recording of the alpha waves, but it goes beyond previous studies in the field [21, 22].

In addition, an analysis of the different sources of noise that had affected the measurement and the ways to reduce them has been done, and some suggestions about the future work in this project presented.

Table of Contents

1. Introduction

Magnetoencephalography (MEG) is a powerful tool to get a better understanding of how the brain works by analyzing the magnetic fields generated by the current flow of the neurons. MEG is useful in functional imaging due to its high temporal resolution but suffers from a lack of precise structural localization, which will be solved with a new technology currently in development at Chalmers. The low amplitude of the MEG signals recorded was a not affordable problem until the use of Superconducting QUantum Interference Devices (SQUIDs). In this project we will also demonstrate that using high critical temperature SQUID fabricated at Chalmers can overcome low critical temperature SQUIDs. Tarte *et al.*, at [20] have created a model to explain his experiments using a brain tissue slice and compared the results using a low-T_c SQUID, showing that the High –T_c SQUID is much more sensible. Our objective is the same but dealing with greater distances between the source of the signals and the detector because we will be performing *in vivo* recordings, as opposed to *in vitro*. The minimum distance between the source and the detector in this case is determined by the thickness of the skull and the cerebrospinal fluid surrounding the brain. Typical source-sensor spacing will therefore be about 1 cm. This distance is, however, shorter than the state-of-the-art in regards to low-T_c SQUIDs, which are limited to 2 cm spacing or more. Some simulations have been done with the aim to determine the order of magnitude of the future measurements, showing coherent results and better resolution than low-T_c SQUIDS *a priori*.

Alpha waves have been chosen because of their high intensity in comparison to the other brain signals. Measuring this type of signals is the first step when dealing with the signals from the brain. Further developments of the detector may allow using the system to detect the rest of the brain signals.

1.1 Outline

In the first part of the thesis a theoretical view of the project is done. The physics of the SQUID and the biological sources of the magnetic signals from the brain are described, in order to understand the background of the MEG recordings. In the following chapters a review of MEG experiments to the date is done, and the design of the experiments of the project is presented. In the last part the results are presented, discussed and compared with the references. Finally some conclusions are presented and future work is proposed

1.2 EU-FP7 project: The MEGMRI-project

This thesis is a part of the EU project FP7. The purpose of the MEGMRI-project is to develop and validate hybrid MEG and magnetic resonance imaging (MRI) technology that will allow simultaneous structural and functional imaging of the human brain. This development will improve the localization accuracy of MEG and simplify workflow, as no high-field MRI will be necessary. Safety benefits (for patient with pacemakers and other implants, for pregnant women, for infants) are also obvious[1].

This task requires many steps, and one of them requires an understanding of how the MEG recordings will look like. This step will be done in this research project.

---

1 More information can be found at https://wiki.tkk.fi/display/megmri/The+Project)

2. Theory

In this part of the project the physical aspects lying behind the SQUIDs are explained, also their parameters and the noise sources that affect them. To understand the origin of the magnetic signals recorded a brief description of the biological origin of neuron currents is given, and also the principal aspects about alpha waves. To end this chapter some general concepts about magnetoencephalography measurements are presented, together with the explanation of why high-T_c SQUIDs are useful to this purpose.

2.1. SQUIDs theory

To understand how the sensors used in this thesis work it should be clear what is the superconductivity and its main characteristics.

2.1.1. Superconductivity concepts

Superconductivity is a property exhibited by some materials under certain critical temperature, and it's characterized by zero electrical resistivity when applying a current and there is no magnetic field present. In addition, if the superconductive materials are placed in a region of space where there is a magnetic field present, they create a set of super currents that create an opposite magnetic field that cancels the external one. This is known as the Meissner effect.

Furthermore, a classification of the superconductive materials is done according the way how the Meissner effect takes place on them: in type I superconductors the superconductivity state disappears when a critical magnetic field is reached, by the other side, type II superconductors have a gradual transition from superconductivity to normal state, and have two critical magnetic fields, H1 where the magnetic field starts to get into the material, and H2 where the superconductivity state is finally destroyed.

The BCS microscope theory states that pairs of electrons with opposite spin can attract each others (named Cooper pairs) as a result of a virtual exchange of phonons, only if the energy difference between the electron states is less than the phonon energy. [3] The Cooper pair net spin is zero so they behave as bosons, all occupying the lowest energy level. For the electrons to form a Cooper pair a length scale factor (coherence length) is defined. This is a long-range parameter that depends upon the material and has values from few nanometres to few micrometers. This theory can explain the interaction mechanisms involved in low temperature superconductors, but not in high temperature superconductors, the ones used in this project.

Another effect in superconducting materials is the flux quantization. In type II superconductors below the critical magnetic field H2 and above H1 the flux penetrates the material in units of the flux quantum Phi_0=h/2e = 2.07 x 10-15 Wb, were "h" is Planck´s constant and "e" is the electronic charge. Flux quantization can be demonstrated mathematically showing that the macroscopic wave function of a Copper pair must be single valued in going once around a superconducting loop.

In this project the superconducting materials used for the fabrication of the sensor have been high critical temperature superconductors, a brief explanation of their properties can be seen bellow. In addition, to comprehend completely the physical phenomena behind SQUIDs the Josephson effect is explained.

High critical temperature superconductors

High critical temperature superconductors are the superconductors that have the critical temperature above 30 K, and their intrinsic behaviour is not completely explained by any theory at the present moment. In this project yttrium barium copper oxide ($YBa_2Cu_3O_{7-x}$), or more commonly YBCO, will be used. YBCO is the most common high critical temperature superconductor used because has a critical temperature of 93K, that makes possible to cool it using liquid nitrogen (at atmospheric pressure boils at 77 K), avoiding the use of liquid helium that is more expensive and that tends to form solid air plugs when piping. YBCO is a copper oxide with a perovskite crystal and due to its high degree of anisotropy the London penetration depth has very different values a long the different axis (130 nm in a-b plane, 800 nm in c plane). The same happens with the coherence length (2,5 nm n a-b plane, 0.4 nm in c plane), resulting in larger disruptions on the current transport because of thermal fluctuations and defects on fabrication.

The Josephson effect

In 1962, Josephson predicted the tunnelling of Cooper pairs through a thin barrier separating two superconductors (Josephson junction). Josephson showed that the current flowing through that barrier was equal to:

$I=I_0 \sin(\delta)$ (5)

where $\delta = \phi_1 - \phi_2$ is the phase difference between the condensates in the two superconducting electrodes and I_0 is the critical current. The critical current is the maximum current that can flow with zero resistance. Josephson junctions are used in quantum-mechanical circuits, such as SQUIDs, because the Josephson effect is highly sensitive to the magnetic fields in its vicinity.

2.1.2 SQUID device parameters

The Superconducting Quantum Interference Devices (SQUIDs) are the most sensitive detectors of magnetic flux known. The device performance lies above the two physical phenomena explained above; flux quantization and Josephson tunnelling [1].

There are two basic SQUID types depending on the number of Josephson junctions that have inside the superconducting loop; the dc SQUID with two junctions and the Rf SQUID with just one. In this project dc SQUIDs has been used because it is easier to fabricate them and they are more sensitive than the Rf SQUID. The dc SQUID is made of two Josephson junctions connected in parallel forming a superconducting loop. (See Figure 1)

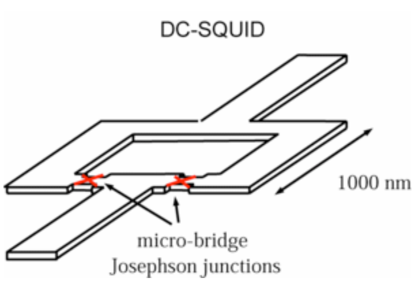

Figure 1. DC-SQUID

As seen in the figure 1, an applied bias current will split in the two circuit branches with the same value, if there is no external magnetic flux applied. If an external magnetic flux is applied (using a coil attached to the chip where the SQUID is bounded) then screening currents will be induced in order to generate a magnetic field to cancel the external one due to the Meissner effect. When the combination of currents (bias and screened) is over the critical current, the Josephson junctions become resistive and one flux quantum can go into the loop by reversing the screening currents, keeping the flux in, since it requires less energy than ejecting it. The maximum critical current is obtained for a flux $\phi = n \cdot \phi_0$ and the minimum $\phi = (n + 1/2) \cdot \phi_0$. In order to do measurements using the SQUID as a gradiometer or magnetometer, a flux modulation is obtained by changing the bias current, resulting in a voltage modulation across the SQUID. To operate the SQUID in order to measure at low frequencies it should be in a flux-locked feedback loop. Feedback is used because it linearizes the response of the SQUID to the applied flux, and because of this allows detecting very tiny changes of a flux quantum. [1]

There is another SQUID classification according to the superconductive material used in their fabrication: Low-T_c SQUIDs if they are fabricated using conventional superconductive materials (that must be operated using liquid helium), and high-T_c SQUIDs if they are fabricated using high temperature superconductors, like YBCO. Practical differences of these two types are explained in detail in the discussion part.

Finally, the last consideration when talking about SQUIDs is their layout configuration. The effective area of a SQUID is limited; therefore to enhance the signal measured to be able to use it for practical applications a large input coil (pick-up coil) has to be coupled to the sensor. Depending on the configuration of the pick-up coil we can have two different SQUID sensors: Magnetometers, which have a large pick-up loop that fits all the area of the chip, and gradiometers, where two or more magnetometers are placed in series or parallel in the same chip. In low-T_c SQUIDs the input coil can be integrated onto the SQUID chip in a separate superconducting layer, but in High-T_c SQUIDs this is difficult to accomplish.

2.1.3. Noise in dc-SQUIDs

There are at least two main important sources of noise in this type of SQUID: 1/f and thermal noise. 1/f noise, also known as flicker noise, it's caused by two factors; The first one is the motion of vortices trapped on the SQUID, and it is caused by trapping of fluxons while cooling the SQUID on a non-zero magnetic field environment. If the thermal energy it's enough large, the vortex can overcome the pinning energy and jump between two or more adjacent pining sites inducing a change in the flux, resulting in adding noise to the measurements. This kind of noise can be seen as a random telegraph signal in the SQUID output, and can be reduced by optimizing the thin-film growth (i.e. improving the quality of the film) [4] or by cooling in an extremely shielded environment. The second one is the fluctuation of the critical current in the Josephson junctions and can contribute in two ways to the dc SQUID noise; the in-phase mode where the critical current of the two junctions fluctuate in-phase and produce a voltage across the SQUID, and the out-phase, where the two fluctuating critical currents produce a current circulating across the SQUID loop.[1] This type of noise can be reduced or even eliminated by using a reversing bias readout scheme (AC bias readout mode). This noise is more high at low frequencies, and that's why it's so disturbing when measuring biomagnetic signals, in this project we'll measure *in vivo* alpha waves that are in the bandwidth of 8 to 13 Hz, but other brain signals like delta waves can go from 1 to 4 Hz. Thermal noise is due to thermal movement of the charge carriers in a conductor, and has an appreciable effect for high-T_c devices like the ones used in this project. This noise can destroy the quantum interference if it reaches 20% of the value of the critical current. [1] This can happen if the temperature is large enough or if Ic is small enough. Mathematically expressed: $I_{th} = \frac{2\pi \cdot k_B T}{\Phi_0}$, where Φ_0 is the Josephson coupling.

$\gamma = \frac{I_{th}}{I_c}$, if $\gamma \leq 0.2$ the critical current is destroyed.

These currents will also generate a flux noise that must be less than one flux quantum in order to be able to do the measurements.

2.2. Neuron currents, neuron magnetic fields, alpha waves

In this section the basic biological concepts to understand the origin of the biomagnetic signals is showed. The advantages of MEG over other traditional systems to study brain activity are presented, as well as the numbers and approximations assumed to do the simulations of the neuromagnetic fields. Physiological details about brain alpha waves are also presented.

2.2.1. The brain

The brain is the most complex organ of human body; it contains about 10^{10} neurons and 10^{14} synapses [5,6], so it's easy to understand why it remains being most unknown. Lots of studies had been carried out, and more should be done in order to answer all the questions regards to the brain.

Until now, the common ways to study brain performance were using PET (positron emission tomography) combined with MRI (magnetic resonance imaging), but this method has less temporal resolution than MEG (hundred milliseconds in contrast to milliseconds for MEG) because it depends on changes in blood flow, it's very expensive because of the radioactive tracers used in PET technique, very hard to be reproducible, and not 100% harmless because of the low dose of radioactivity of the positron tracers (with ionizing radiation energies) used while the exploration. To study the brain activity also EEG (electroencephalogram) is used, but it lacks from enough sensitivity in spatial resolution due the distortion of the EEG signals caused by the different electrical properties of the head tissues (the scalp and the skull, mainly) [9]. Like EEG, MEG measurements are non-invasive, 100% safe (no ionizing radiation is used) and have high temporal response, typically about 1 ms. The final prototype of the MEGMRI-project will combine MEG with MRI, bringing a powerful tool to study from a new point of view the human brain.

Mental activity in the brain is associated to the current flow from and to neuron cells, and therefore a basic understanding of their physical behaviour must be explained to fully comprehend the nature of the signals that will be recorded from them.

2.2.2. The neuron currents: dipole approximation

Neurons are one of the cells that form the nervous system and are specialized in receive, process and transmit action potentials. Neurons are structured in three different parts: The main body of the cell, called soma, contains the nucleus and organelles and processes the information received by the dendrites, that are small ramifications that grow from the soma and connect other neurons via synapses, and the axon, that arises from the soma and grows to other neurons, organs or to another dendrites, and carries away the action potentials from the soma.

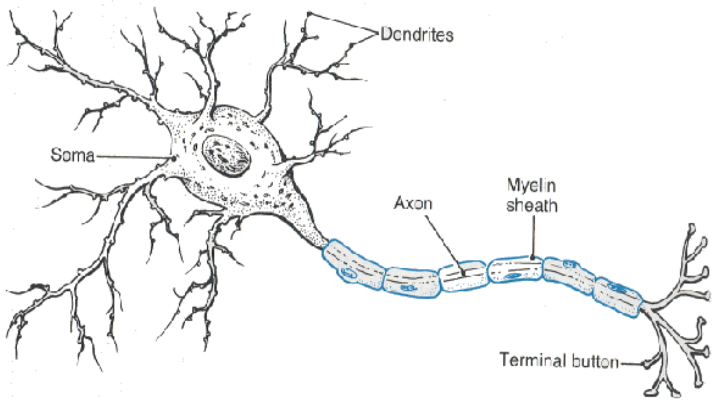

Figure 2. The neuron

Neurons soma have a diameter around 6 to 120 micrometers [7] and are surrounded by a lipid bilayer containing many ion channels and ion pumps (mainly sodium, potassium, chlorine and calcium) that are responsible for the action potentials that are used to transmit and receive signals from other neurons. During activation, the resting potential changes rapidly resulting in a directed flow of charge that gives rise to magnetic fields. Since different types of ions simultaneously take part in this flow, the resultant field is the sum of multiple small magnetic fields. The currents at resting membrane potential do not contribute to the external magnetic field due to the radial symmetry of the membrane and their weakness in comparison to the activation potentials. Neuronal excitation is conducted over great distances with high velocity by action potentials. These are short lasting and caused by rapid changes in membrane conductivity. Two features are responsible for difficulties in detecting the magnetic fields of the action potentials [8]:

- Current dipoles at the region of the action potential generation are directed forward and backward, the result being a quadrupolar magnetic field that has amplitude much weaker with greater distances in comparison to a dipolar magnetic field.

- The short duration of the action potential makes temporal summation limited. Despite of that, the chance for summation increases if neurons in a limited region are synchronously activated.

Generally, the magnetic sources are distributed along the brain cortex; however, activation of even large numbers of cells can often be assumed spatially small and can be modelled by a point equivalent current dipole. Usually, the current-dipole moments required to explain the measured magnetic field strengths outside the head are on the order of 10 nA·m, therefore, about a million synapses must be simultaneously active to be detectable. As an example, auditory evoked fields (AEF) show fields that typically yield to equivalent current dipole magnitudes in the range 20 to 80 nA·m. It was showed that the current dipole density in the brain tissue is nearly constant and ranges from about 0.5 to 2 nA/mm^2, which for AEF dipole magnitude translates to the order of 1 cm^2 of activated cortical tissue. [8]

2.2.3. Signal Analysis of Brain waves

Electrophysiological brain signals reflect the superposition of the magnetic or electric fields caused by a great number of simultaneous intracranial processes. These signals can be classified as spontaneous when are not related to any apparent external event, or event-related when the signals are related to stimulus or the execution of a movement. In addition, these signals can be also divided into transient, if they show singular deflections or oscillatory when they show repetitive deflection activities. Brain oscillations are divided according to their frequency into various bands, which are labeled with Greek letters following the history of their discovery (alpha, beta, gamma, delta and theta waves) and cover the frequency range of 2 to 100 Hz. The alpha rhythm (8 – 12 Hz) is the strongest over parietal and occipital parts of the skull, and is reduced by opening the eyes (Berger effect) as well as by visual stimuli and visual imagery.

In spite of intensive research on the electroencephalogram (EEG) over more than 70 years, there is still no generally accepted theory on the functional meaning of occipital alpha waves. Recent studies suggest that alpha waves are part of a long-range neuromodulatory network, not part of the visual processing network [9].

2.3 Magnetoencephalography measurements

Magnetic brain signals detected using MEG arise from the flowing of the currents of the pyramidal neurons, which are mainly localized in the brain cortex. Because of that, MEG signals can be measured on the surface of the head. The cortex (Fig 3a) contains well-aligned pyramidal cells that consist of dendrites, cell bodies and axons. The density of these cells is approximately 10^5-10^6 cells / 10 mm^2 of cortex [10]. The dendritic currents due the depolarization / hyperpolarisation of this cells flows roughly perpendicular to the cortex, however, the cortex is convoluted with numerous sulci and gyri and, so depending on where the cell stimulation occurred the current flow can be either tangential or radial to the scalp surface (Fig. 3b, 3c, 3d). Current flow within a single cell is too small and cannot produce observable magnetic fields outside the scalp, so for fields to be detectable it is necessary to have nearly simultaneous activation of a large number of cells, typically 10^4 to 10^5 [11].

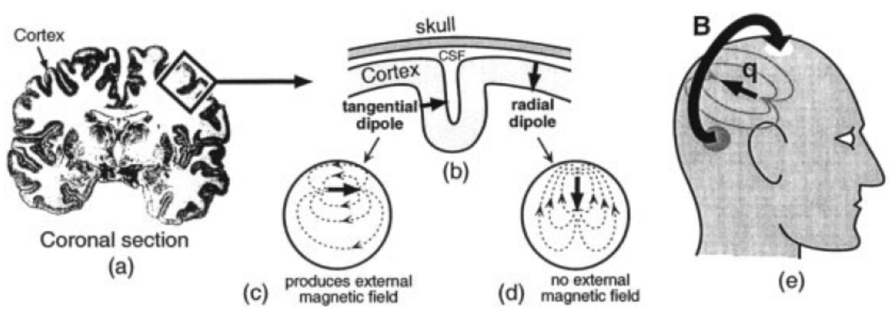

FIG. 3. Origin of the MEG signal. (a) Coronal section of the human brain. Cortex is indicated by dark colour. (b) Sulci and gyri in the cortex. (c,d) Radial currents will not produce magnetic fields outside the head.(e) Magnetic fields due to cortical sources will exit and reenter the scalp [11].

MEG measures the distribution of magnetic fields on the two-dimensional head surface. However, the required information is usually a three-dimensional distribution of currents within the brain. Unfortunately the field inversion problem is non unique and MEG data must be supplemented by additional information, physiological constraints, or mathematical simplifications.

Modern MEG systems employ low-T_c SQUIDs because they are the most sensitive magnetic field detectors. Until 80's the biomagnetic measurements were carried out using single channel magnetometers with pickup and compensation coils, but this limited their use to simple local measurements of the neuromagnetic signals. The first multi-SQUID magnetometers had 4-5 channels on an area of only few cm, and modern MEG systems cover the whole head using an array of hundreds of SQUID detectors that surround the head. [10] This configuration allows mapping the magnetic brain activity in all brain regions. Usually to minimize the effects from ambient electromagnetic radiation sources and prevent typical urban magnetic noise from overwhelming the highly sensitive detectors, MEG measurements are performed inside a magnetically shielded room (MSR).

2.3.1. The high-T_c advantage

The main purpose of constructing a new type of MEG system using high-T_c SQUIDs is due to improve the sensitivity of them by reducing the distance of the surface of the head to the sensor by less than a millimetre. This reduction increases the signal strength by more than an order of magnitude (see Fig 6 in Results section), and it's possible because of the lower thermal insulation required by high-T_c SQUIDs, in opposition to the traditional ones (low-T_c SQUIDs), that operate at much lower temperatures and their minimum stand off is about few centimetres. Furthermore, using high-T_c SQUIDs also would reduce global costs because of various reasons; The system uses liquid nitrogen instead of liquid helium which is much cheaper, dewars used for high-T_c sensors are also cheaper and easier to handle than traditional ones and the downtime related to repair or replace a high-T_c SQUID sensor is easier and faster than for a low-TC sensor. (few hours in contrast to two days)

3. Experiments to date

Before going further into the methodology details of this study, some experiments related to the field will be presented.

TARTE et al. *High-T_c SQUID systems for magnetophysiology*

In this paper the authors detected neuromagnetic fields of brain tissue slices, after electrical stimulation. In addition, they constructed a model of electrical activity in a hippocampal brain slice so they can determine the neuromagnetic field as a function of position and distance from the tissue. The authors use the dipole approximation to model the magnetic field. They show that high-T_c SQUIDs have superior signal to noise ratio compared to a low-T_c system.

OKADA et al. *Genesis of MEG signals in a mammalian CNS structure*

In this study the authors characterize the neuromagnetic signals of guinea pig hippocampal slices, and they compare it with the extracellular field potential to elucidate the genesis of the MEG signals. Their results show that the dipolar component of the intracellular currents is the dominant factor generating magnetic fields, even at a distance of 2 mm from the slice.

DANTSKER, E. et al. *Reduction of 1/f noise in high-T_c dc superconducting quantum interference devices cooled in an ambient magnetic field*

In this paper the authors prove that the low frequency 1/f noise of high-T_c SQUIDs is independent of the magnetic field in which they were cooled, up to a threshold of 33 μT. They also concluded that reducing the line width of the device could lower this kind of noise.

4. Methodology

Before trying to record the alpha waves using a high-T_c SQUID, some experiments have to be done with the purpose to find the best sensibility when doing the biomagnetic measurements. These include; find the SQUID magnetometer with the higher signal-to-noise ratio, find the best place and way of cooling it (low field, shielded environment), and finally find and learn the best way of adjusting it to the working point to be able to operate it reducing as much as possible the noise.

4.1. Materials used

The setup for the SQUID sensor characterization consisted of a Magnicon SEL-1 SQUID electronics, a Stanford Research SR785 spectrum analyser (to do the noise measurements) and a FLUKE function generator. The SQUID is operated using the software “SQUID Viewer” provided by Magnicon, and the instruments are controlled by LabVIEW programmes. The magnetometers and gradiometers tested and used in this project are designed and fabricated at Chalmers University of Technology by the Phd student Fredrik Oisjoen and Dr. Alexey Kalaboukhov. Both types of sensors are built over a 10X10 cm $SrTiO_3$ bicrystal with a 24º misorientation angle using the high temperature superconductor material YBCO. The junctions are grain boundary type.

The measurements have been done in a Radio Frequency Shielded Room (RF-SR) and in a Magnetically Shielded Room (MSR). The first one is shielded against electromagnetic noise at high frequencies and has a background noise around 1 uT, while the other one is shielded against noise in all the frequencies, with a background noise of tens of nT. Magnetically shielded room are constructed using several separated layers of metal alloys with high permeabilities to shunt the external magnetic fields. Usually the materials used to construct shielded rooms are aluminium, mu-metal or a combination of them. Mu-metal is a nickel-iron alloy that has very high magnetic permeability, making it useful to screen low-frequency magnetic fields. This high permeability makes mu-metal very effective at screening static or low frequency magnetic fields. Another type of shielding that also has been used is Bismuth Strontium Calcium Copper Oxide, or BSCCO, which is a high-temperature superconductor. It has a critical temperature of 95 K that is very convenient because when cooling our sensor inside it using liquid nitrogen will expel all the external magnetic field due to the Meissner effect.

The SQUID used for measuring the alpha waves in the project are magnetometers, because of their big pick up loop that allow them to trap more flux. Some of the magnetometers used have been also used to successfully measure the magnetocardardiogram (magnetic fields from the heart).

Before measuring the noise, a brief characterization of all the available SQUID chips for the project was done. The critical currents of each gradiometer/magnetometer were measured, the peak to peak voltage modulation, and if it was possible or not to adjust them to the working point. In addition, the chips were labelled, making easier handling them (see table 1).

To do these measurements, the chip containing the SQUID is glued to a laminated circuit board, and the contacts between the chip and the board are made by wedge bonding. After that, the board is mounted in a dipstick, and a cylindrical BSCCO shield placed around it. A copper shield closes the dipstick. The dipstick is placed inside a dewar designed for liquid nitrogen use. Finally the dewar is surrounded by three concentric cylindrical mu metal shields.

At certain point of time, the setup was improved by placing the whole system described inside a plastic tube serving as vacuum chamber. With this configuration it was possible to pump using an air-pressure driven pump so the temperature could be reduced. This supposed an improvement on the SQUIDs performance for two reasons: The critical currents were increased as the temperature went down (and the pressure up) and the voltage modulation also increased significantly.

NAME OF THE CHIP(*)	CRITICAL CURRENT (μA)	PEAK TO PEAK VOLTAGE MODULATION (μV)	ADJUSTABLE TO WORKING POINT
CSG1	Ic (left) = 220 Ic (right) = 250	V_{mod} =25	YES
CSG2	Ic (left) =165 Ic (right) =200	V_{mod} =20	YES
CSM1	Ic(left)=44 (after pumping) Ic(right)=45 (after pumping)	V_{mod} =20	YES
CSM2	Ic=6,5uA	V_{mod} =30	YES (After pumping)
CSM3	Left SQUID is dead Ic (right)=75	V_{mod} =60	YES (After pumping)
CSM4	Ic=5uA	-	NO
CSM5	Ic=100uA	-	NO (Squid is dead)
CSM6	Ic (left) = 70 Ic (right) = 230	V_{mod} =30	YES
CSM7	Ic (left) = 17 Ic (right) = 21 (after pumping)	V_{mod} =75	YES

Table 1. Chips used during the project. (*) G/M indicate gradiometer/magnetometer on the chip

After the characterization of every magnetometer and gradiometer we proceed to take noise measurements of the different sensors inside a dip-stick, in the RF-SR of the Department of Microtechnology and Nanoscience at the Chalmers University of Technology. The different SQUIDs have been measured in the following configurations conditions.

4.2. Noise measurements in the dip-stick

Some noise measurements have been done with the aim to find the best magnetometer for measuring the neuromagnetic signals. According to the simulations and the literature [8], the value of the magnetic field resulting from the alpha waves is around the pT between 8-12 Hz, so the SQUID sensors should show at least one order of magnitude lower noise for the same frequencies to be able to record these signals.

- Cooling using liquid nitrogen and doing the measurements inside the R.F. shielded room, shielding the detectors using a two mu-metal cylinders and cooling within a superconductive layer of BSCCO: The measures showed big noise in all the detectors (see Fig 6 in results part).

- Cooling using liquid nitrogen and doing the measurements inside the R.F. shielded room, only shielding the detectors with a superconductive layer of BSCCO: The measures also showed big noise in all the magnetometers (see also Fig 6 in results part).

- Cooling using liquid nitrogen and doing the measurements inside the R.F. shielded room while pumping the air out to increase the critical current, shielding the detectors using a two mu-metal cylinders and cooling within a superconductive layer of BSCCO: Again, the different measures presented big noise.

- Cooling using liquid nitrogen outside the R.F. shielded room and doing the measurements inside while pumping the air out to increase the critical current, shielding the detectors using a two mu-metal cylinders and cooling within a superconductive layer of BSCCO: The measures showed less noise, reaching the necessary noise levels for using the SQUIDs to record alpha waves (see Fig 7 and 8 in results part).

In discussion part of the project these differences are analyzed in detail.

4.3. Noise measurements in the cryostat

After finding the sensor with low noise performance, we placed it inside the cryostat to be able to do the brain signals measurements. The cryostat is made of fibreglass to reduce the Nyquist noise generated in conductors, and contains a window at the top where the magnetometer is placed to be as close as possible to the surface of the head. The whole system inside the cryostat is in vacuum to improve heat isolation from the outside. The cryostat does not have any shielding; because of this it is required to do the alpha wave recordings in a shielded environment. This is due to the large difference between the magnetic environmental signals (more than 10^{-4} Teslas) and the neuromagnetic signals recorded (maximum value of 10^{-12} Teslas), this is more than 8 orders of magnitude difference! In this project the "*in vivo*" alpha wave recording measurement have been done inside a mu-metal room at the company IMEGO.

4.3.1. Protocol to measure alpha waves

Locating a single detector is not a problem in the literature since most of the MEG papers refer to multichannel neuromagnetometer equipments, usually with hundreds of detectors, to have spatial information to locate the sources from measurements without moving the instrument.

According to the literature, the alpha waves are generated in the occipital region of the brain (14,15,16,18), so the best place to place the detector is as much closer to the main source of neural currents as possible. Because of the low amplitude of the fields and the cancellation of the currents, we can only detect the orthogonal fields induced by tangential currents. This is the case in the fissures of the brain. The *calcarine* fissure could be a source of magnetic field detection, as concluded in [13]. This fissure has an orientation of 45º with the normal plane, so the detector must be placed orthogonally to the fissure plane, 135º over the normal plane. In the figure 4 we can see the calcarine fissure plane (orange line), and the electrical fields direction of an equivalent dipole (green and yellow lines), the magnetic resultant field is the red line, perpendicular to the electrical field and the calacarine fissure plane. The best place to detect the alpha waves should be in the direction of the magnetic field.

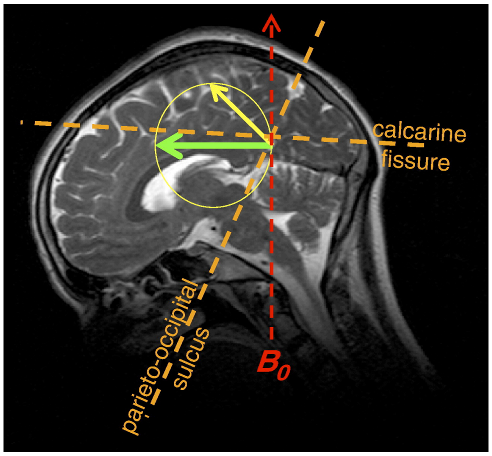

Fig. 4. Best location to detect alpha waves coming from the brain

According to the simulations done, the order of magnitude expected of the recorded signals should be of 50 pT/cm^2 and 1 pT/cm^2 for the detector at 1 cm and 4 cm from the source respectively According to the literature, the range goes from few fT to pT ([14], [15], [16], [17]).

To do the alpha wave recordings is necessary a measurement protocol to be accurate when doing the different recordings, so they can be reproducible. We need to place the detector as close to the head as possible to have maximum strength of the signal. The detector (cryostat) can move over a table, next to a pair of rulers to determine the approximate distance to the head. The volunteer is seating in a chair that is always kept in the same position and three lasers attached to his head ensure that the head is not moving while measuring. The first measurement is done with the head touching the surface of the detector and with the eyes closed in order to have the strongest signal possible (see Fig.5). Then different series of measures are done in order to determine if the detected signals corresponded to alpha waves and not to noise or other body signals. A band pass filter between 0.1 and 100 Hz is used and also an amplifier to acquire the raw data.

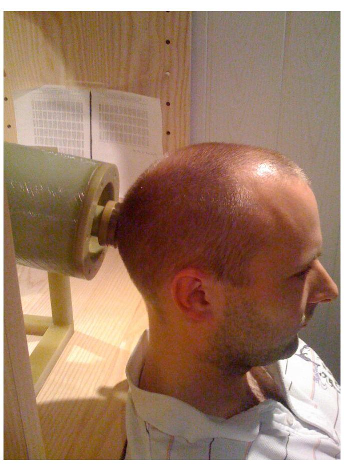

Fig. 5. Alpha wave measurement of volunteer 1

4.4. Cooling methods

The HTS material used in the SQUIDs was YBCO that has a critical temperature of 92K, so liquid nitrogen could be used to cool it down. The way and the place of cooling the SQUIDs have been showed to be crucial when measuring the noise.

It has been observed that cooling in a slow way (pumping liquid nitrogen inside the cryostat with the SQUID sitting at the bottom, for more than 3 minutes) gives better SNR than cooling fast (depositing the SQUID in a cryostat full of liquid nitrogen). The place where the SQUIDs are cooled also changes its performance dramatically. In this project, the best way of cooling consisted of doing it outside the RF shielded room, using two layers of a mu metal and BSCCO shielding. With this configuration it was possible to reach 40 femtoTesla at 10 Hz, that's more than enough to record the magnetic brain signals.

4.5. Working point adjustment (DC, AC bias schemes)

SQUIDs can be used to measure any physical quantity that can be converted in a magnetic flux; their most simple configuration is to use a single pickup loop to form a magnetometer. To read the signal coming from the SQUID electronics, this must be operated in a flux-locked loop (FLL). This means that the signal from the SQUID is sent back through an amplifier and a feedback coil to generate a flux to cancel the flux in the SQUID. This is done to have a linear response of the SQUID to the changes in the magnetic flux. To operate it in FLL mode, the SQUID is biased at working point, which is typically located near the steepest part of the V- ϕ characteristic. Doing this, a small change in the applied flux $\delta\phi$ will produce a proportional change in the voltage, achieving the maximum sensitivity.

Critical current fluctuations can be reduced if the bias reversal technique is used (called ac bias). The idea of this read-out method is that the polarity of the V-ϕ characteristic along the flux axis changes due to a change in polarity of the bias current, whereas no change in polarity occurs for the flux due to an input signal. Because of this the in/out phase fluctuations of the critical current can be eliminated (as an example, see Fig. 11 in results section)

5. Results

5.1. Simulations

The first step in this project was to run some simulations with the aim to have a general idea of the order of magnitude of the neuromagnetic brain signals, modelled as a dipole, detected by a regular sensor outside the head. The dipole approximation has been used because the distance between the source and the detector can be considered as far enough, considering that the sources are point-like. In addition, this approximation is very common in literature when calculating the brain magnetic field of hippocampal brain tissue slices [8].

Using the dipole approximation:

$$B(\vec{m},\vec{r}) = \frac{\mu_0}{4\pi}\left[\frac{3(\vec{m}\cdot\vec{r})\cdot\vec{r}}{|\vec{r}|^5} - \frac{\vec{m}}{|\vec{r}|^3}\right]$$

, and if the dipole is pointing the detector, $\vec{m} = m\cdot\hat{e}_x$

then we can run the simulations using:

$$B(x,y,z) = \frac{\mu_0}{4\pi}\left[\frac{3\cdot m\cdot x^2}{\left(\sqrt{x^2+y^2+z^2}\right)^{5/2}} - \frac{m}{\left(\sqrt{x^2+y^2+z^2}\right)^{3/2}}\right]$$

For the magnetic moment we took that $m=10^{-9}$ A/m^2 for a surface activation of 40 mm^2, from [13]. Then we evaluate the equation for different points of the space, considering the area of the SQUID detector of 1 cm^2. The results can be seen in the fig 6.

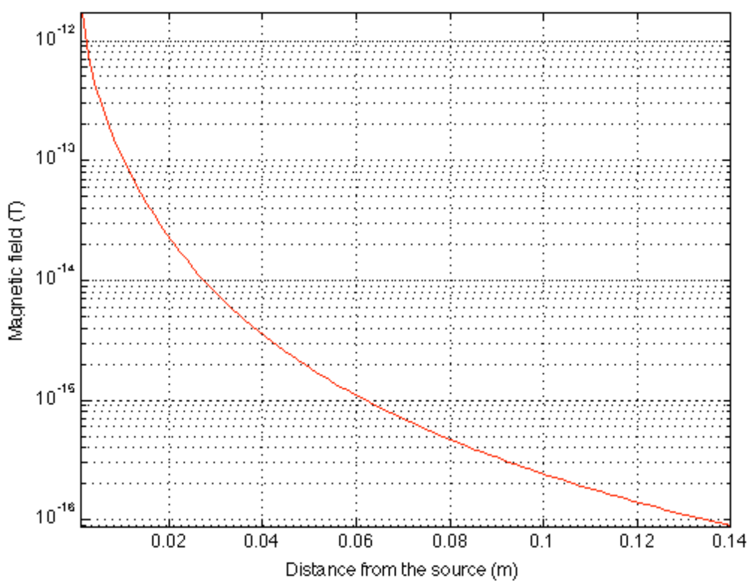

Fig. 6. Results from the simulation considering neuromagnetic signals as dipoles.

This simulation shows that neuromagnetic fields have an order of magnitude of pT in the typical distance source-detector (1mm to 4 cm), which is confirmed by the values consulted in the literature.

Another fact we can extract from the simulations is the best performance of high-T_c SQUIDs in comparison to the low-T_c ones, because of their small stand off. In figure 7 the signal ratio between typical MEG sources at different distances from the detector has been plotted. We can observe that the magnetic signals coming from the brain are reduced by an order of magnitude in short distance (less than 5cm), that's why the stand off is so important to reduce. The detector performance for the deepest sources is not very good for this kind of detectors, despite of that, the main MEG signals from the brain arise from the cortex. (See also Fig. 3).

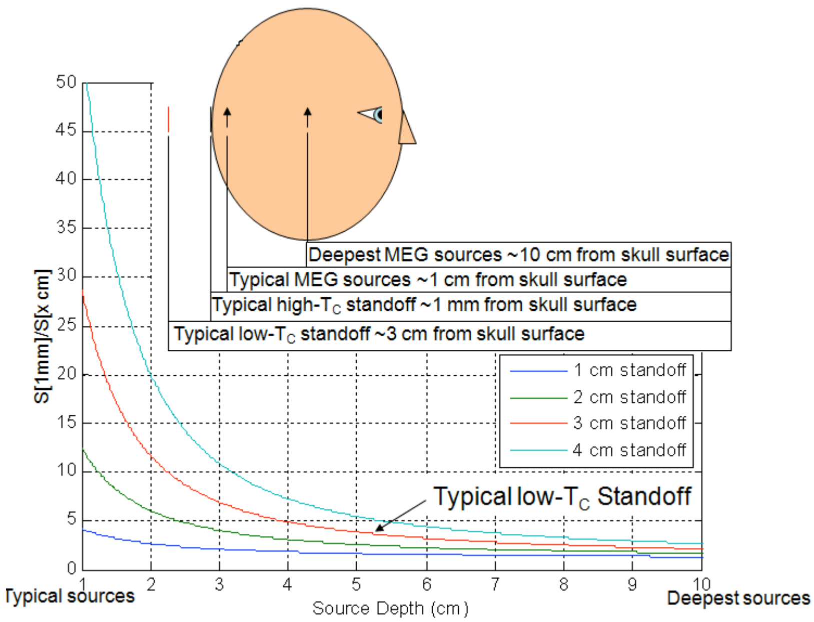

Fig.7 Results from the simulation considering neuromagnetic signals as dipoles from sources at different distances.

5.2. I-V characteristics and voltage modulation

The results from the I-V measurements of a sensor used in the project can be seen bellow. Observing and analyzing these curves we can see determine the voltage modulation due to applied flux near the critical current.

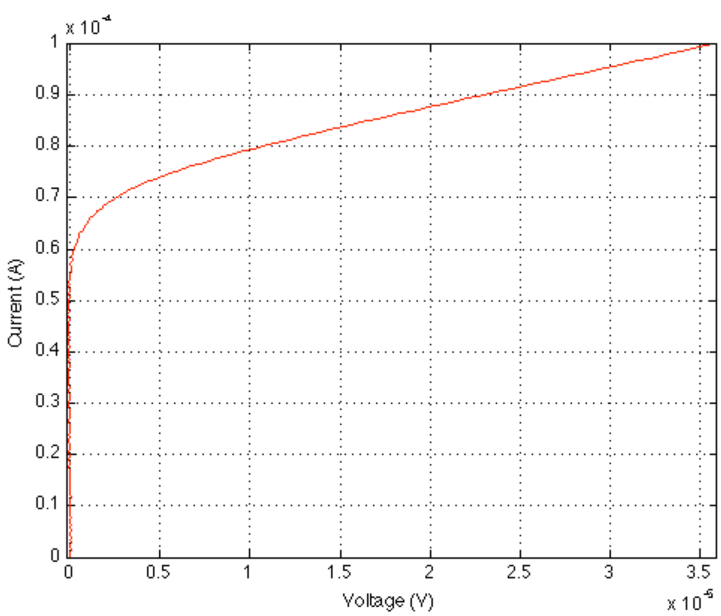

Fig. 8. Measured I-V curve for a magnetometer

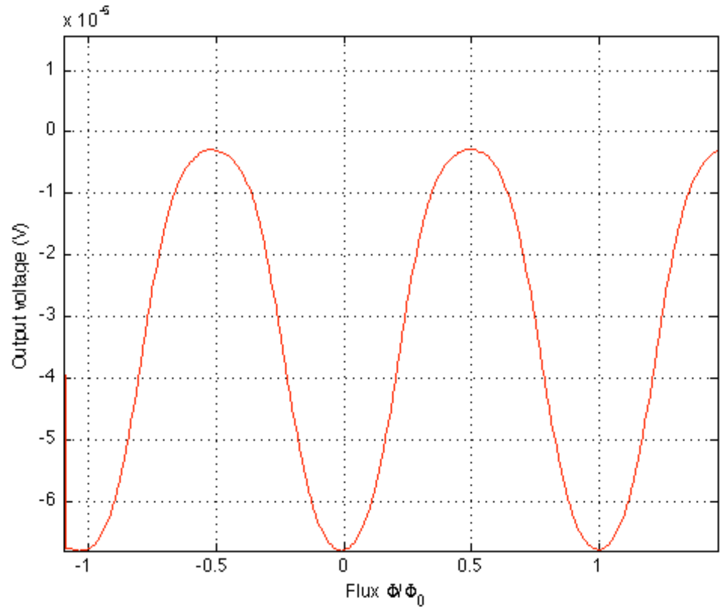

Fig. 9. Measured voltage modulation created by an applied flux

5.3. Noise measurements results

Many measurements have been done in order to find the best sensor and the best way to operate it. Bellow the most representative data is listed, with an explanation of the problems as well as the solutions found to each one.

5.3.1. At Chalmers

The first measurements were done using a gradiometer, and large amount of noise was observed. As a result of this some actions were taken:

- Look for noise sources near the SQUID, like magnetized surfaces, electrical devices that could be interfering: nothing was found.

- Change the feedback coil of the chip where the SQUIDs were bounded to improve the coupling: noise was still there.

- Change of the BSCCO shielding, thinking that maybe it was damaged, but it showed the same level of noise (see figure 10). The results illustrated that there was almost the same level with and without any shielding.

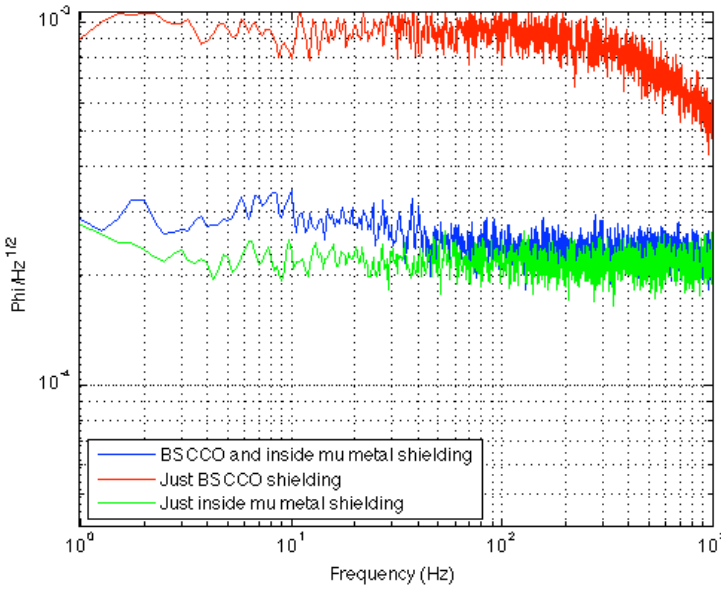

Fig 10. Noise measurement inside the RF shielded room, with and without the two mu-metal and BSCCO shielding for different gradiometers

Note that the y-scale of the figure 10 is in units of Phi/Hz$^{1/2}$ and not in units of Tesla/Hz$^{1/2}$ as we might expect. The reason for this is that we do not have the conversion factor for the gradiometers to convert the units of flux quantum ϕ_0 trapped by the pick up loop to units of magnetic field. For the magnetometers we have a conversion factor of 5 nT/ϕ_0. This conversion factor was obtained in previous experiments, applying different values of known magnetic fields and measuring the flux quantum respectively.

- Pump the air out of the dip-stick, trying to increase the critical current of a previous SQUID that worked in an older series of measurements where a magnetocardiogram was successfully recorded (MCG). This helped because the SQUID could be operated in FLL mode, but it still show higher noise than before. Repeating the same procedure but cooling slowly the SQUID outside the shielded room and measuring inside reduced the noise by an order of magnitude (see fig 11).

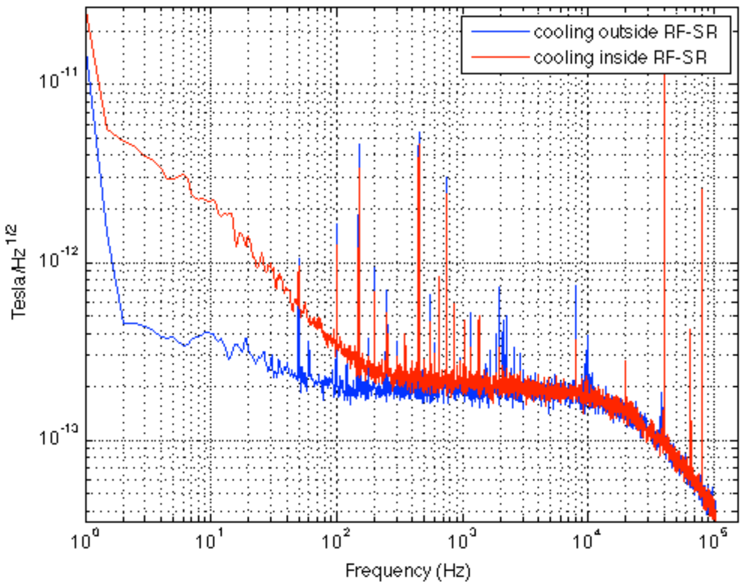

Fig 11. Noise measurement cooling outside the RF shielded room but measuring inside vs cooling and measuring inside, with two mu-metal and BSCCO shielding.

Unfortunately, that SQUID (CSM2) was completely destroyed when moved to the cryostat. For that reason a new magnetometer was build that also showed excellent performance.

5.3.2. At IMEGO

The last noise measurements and the alpha wave recording were done inside the magnetic shielded room of the company IMEGO. Cooling was done in a slowly way, using a Helmholtz coils to cancel the low external magnetic field that was present inside the MSR. The results showed an excellent signal-to-noise ratio, with less than 30 fT/√Hz at 10 Hz, as can be seen in the Fig. 12. This allowed starting the alpha wave recording in the same experimental conditions.

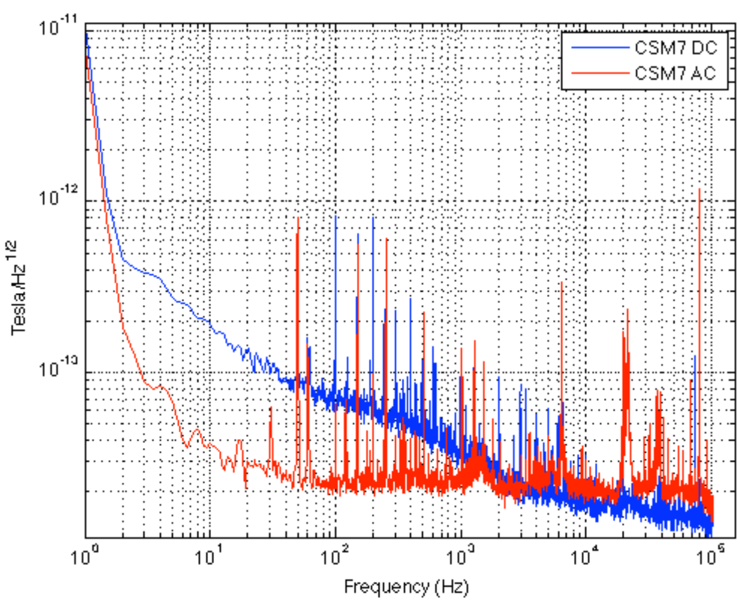

Fig 12. Noise measurement of magnetometer CSM7 inside IMEGO shielded room.

5.4. Alpha wave recording at IMEGO

The first measurements were thought to identify some brain signal, to check that the set-up was done correctly before trying to measure the alpha waves. The cryostat was set at the minimum distance from the head of the volunteer and the measurements were performed with the eyes closed and at different head orientations, beginning with the position 1 for the head aligned with the detector, and then at positions 2, 3, 4, 5 rotating the head a few degrees for each position. After that a blank measurement was done with nobody in the MSR. A variation of the recorded signal was observed between the two states for the different head positions, showing that some biological signal was being recorded. (See Fig. 13,14,15,16,17)

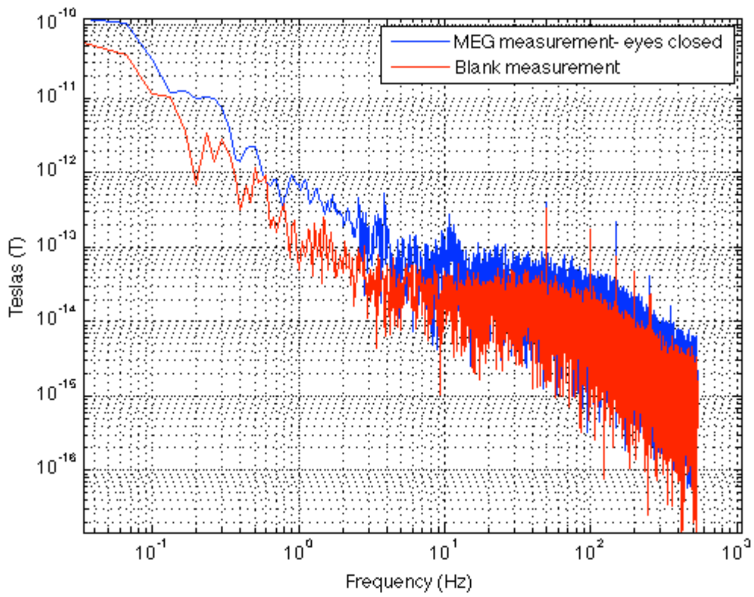

Fig 13. MEG measurement using CSM7 versus blank measurement. Position 1.

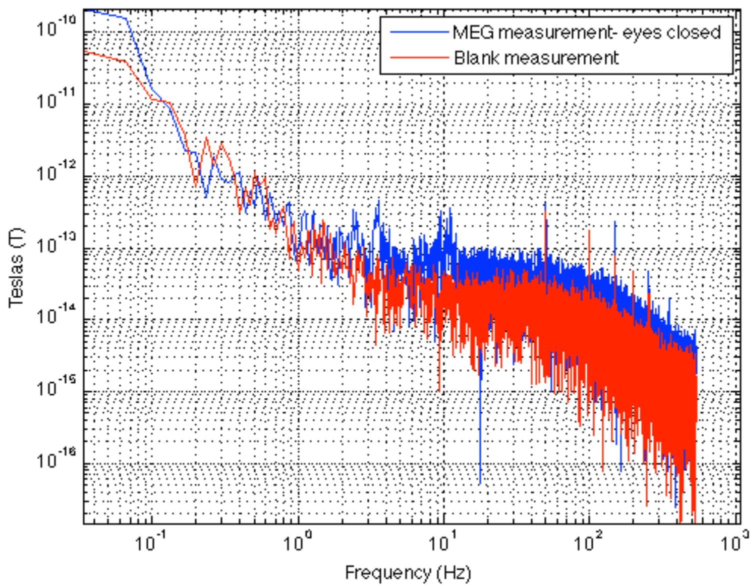

Fig 14. MEG measurement using CSM7 versus blank measurement. Position 2.

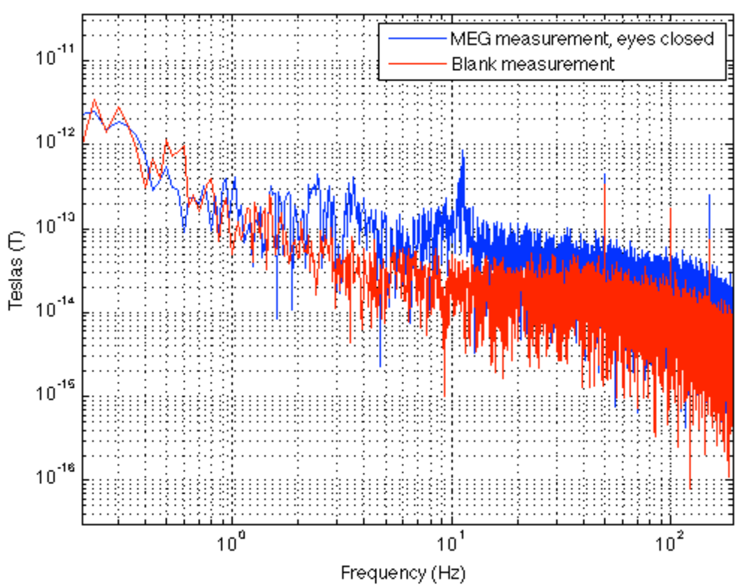

Fig 15. MEG measurement using CSM7 versus blank measurement. Position 3.

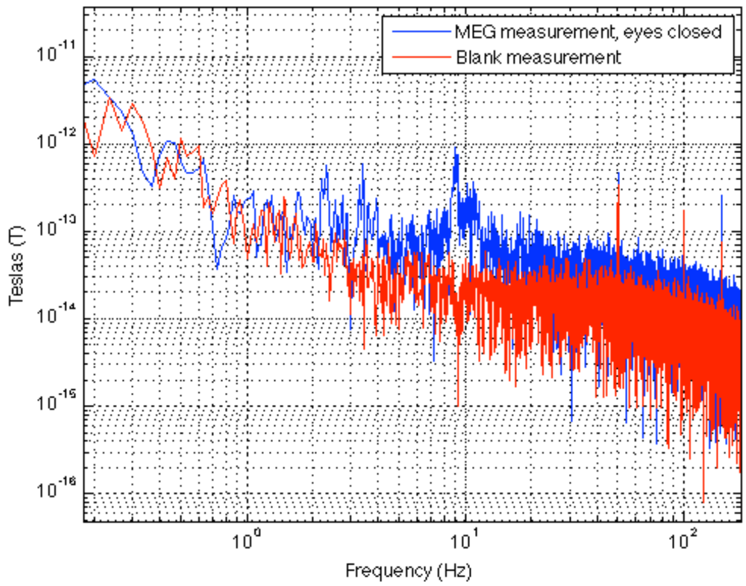

Fig 16. MEG measurement using CSM7 versus blank measurement. Position 4.

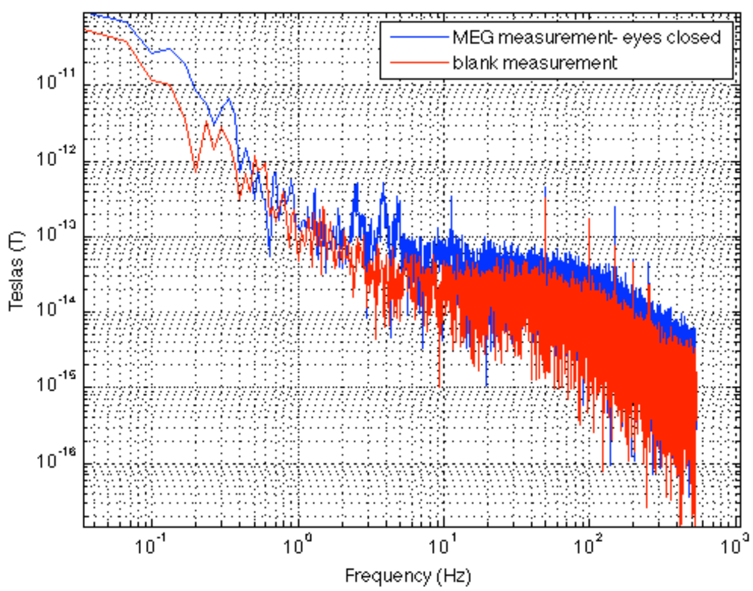

Fig 17. MEG measurement using CSM7 versus blank measurement. Position 5.

Observing the data recorded we could conclude that the higher signal was obtained for the position 4.

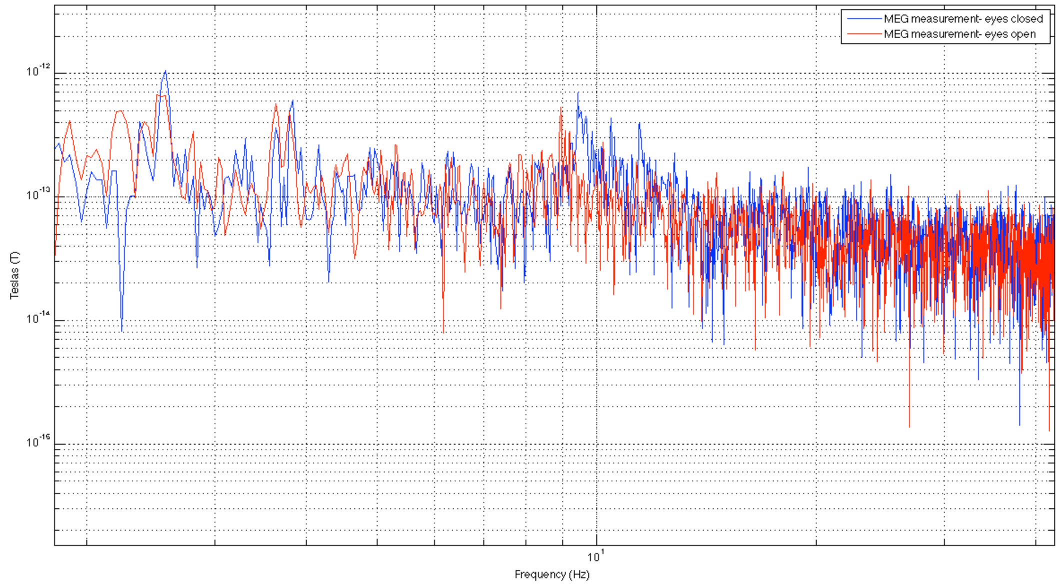

Fig 18. MEG measurement using CSM7 versus blank measurement. Eyes closed vs. Eyes opened.

No such big differences where observed between the measurements done with the eyes closed versus the eyes opened. This fact is discussed in the point 6.4.

Unfortunately the sensor CSM7 was destroyed after recording these measurements. Therefore more measurements results could not be added to this project due to lack of time.

6. Discussion

Although the final step of this project was record brain alpha waves using high-T_c SQUIDs, many other results and therefore discussions had arise during the research through the final objective. These discussions are described bellow.

6.1. How cooling is important

After a series of extremely noise measurements, the cooling procedure of the SQUIDs was revised and different ways of performing it were studied (explained in the methodology part). Once we analyzed the results, we first discovered that the cooling-down velocity was crucial to improve the final results. Cooling-down in a slowly way (pumping nitrogen at low pressure into the liquid nitrogen dewar) reduced the 1/f noise in the measurements. This could be explained by less flux trapping in the body of the SQUID, reducing at the same the motion of the vortices. The second interesting discovery was that changing the place where the SQUIDs were cooled was also essential. Cooling outside the RF-shielded room improved the SNR by an order of magnitude. A possible reason for that would be that a low-noise-source is inside the RF-shielded room but it has not been found.

6.2. How sensor affects

The magnetometers and gradiometers used in this project (see table 1) showed extremely different performances, although the most part of them were fabricated using the same materials and the same technique. This is due to the random processes during the fabrication method. According to the literature, third order gradiometers can be used in unshielded environments with good SNR results. Despite of that, the SQUIDs used to measure the alpha waves were magnetometers, mainly because of their big pick up loop that can acquire much more signal than any gradiometer. This is crucial in this project because of the low amplitude of alpha waves signals. In addition, although their fabrication technique is hard, is easier to do than third order gradiometers using high-T_c materials.

6.3. Noise issues

Noise measurements are always present in every experimental measurement, but they have big importance in this project, because of the low amplitude of the signal compared to the magnetic environment signal. Because of that most of the time of the project has been dedicated to reduce it. This is clearly the worst part of HTS in front of LTS. The question to be answered if it the advantages brought by using HTS overcome their weaknesses.

6.4. Alpha wave recordings

Observing the different figures (13-17) we can conclude that brain signals were successfully recorded, and that are more prominent in some positions than in others. Concretely in the position 4, that is close to the position O2 (in the 10-20 international reference system, see Fig 19.) a typical alpha wave source according to medical expert [18].

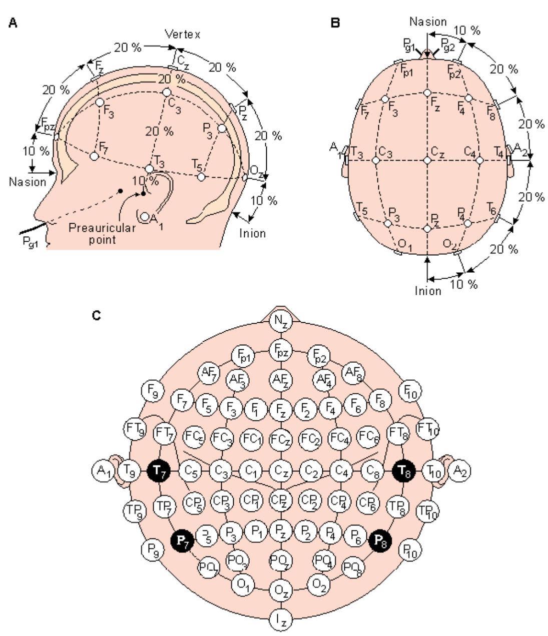

Fig 19. 10-20 international system, the standard naming and positioning scheme for EEG applications.

According to the alpha wave recordings acquired using EEG from [19], a higher peak near 10 Hz is observed, that makes sense to the results obtained. In addition, we can see in all the figures smaller peaks between 2 – 5 Hz that correspond to slow alpha waves, according to medical expert [19].
The small difference between the signals recorded with the «eyes closed state» in comparison to the «eyes opened state» could be explained by the lack of enough visual stimuli. This is can also be seen at [20], where the difference in amplitude between the two states is 3 times bigger for the «eyes closed state». Despite of that, some more measurements should be done to fully confirm that alpha waves were recorded properly.

6.5. Future work

The final stage of this project is to build a working prototype of a hybrid MEG MRI system. Still is a long way to go, but this project showed that even with a single magnetometer the tiny brain signals could be recorded.

The next step in this project would involve doing more measurement using the same experimental setup to confirm that alpha waves were recorded and that the results are reproducible. These results will lead to publish an article because it is the first time that brain alpha waves have been measured and quantified using this kind of sensor. Previous studies showed that measuring audio evoked fields (AEF) from the brain using the same kind of sensors was possible [21, 22], but none of them went beyond that. Future improvements in this project can be done using SQUIDs with multilayer configuration. The expected results of this major improvement is that the signal to noise ratio will be increased by, at least, one order of magnitude, making them as sensitive as the low-T_c SQUIDs.

At long term, and to be able to measure and localize the exact brain region that is activated, more detectors should be used. This implies that the electronics should be extended by as much as sensors as possible to be able to record at different head locations at the same time. This way will also allow reducing the error in the measurements because of the possibility to do correlation between the detectors. Also a new cryocooler should be designed/bought in order to fill all the SQUIDs and still be able to place the head of someone inside.

7.Conclusions

In this project a high temperature-conducting SQUID has been used to observe and record a specific type of brain signals, the alpha waves. The aim of the project was to perform a “proof of principle”, proving that this type of recordings were possible, and it has been accomplished.

It has been showed that using this type of detector brain signals can acquired at a decent signal-to-noise ratio. It has also been found that the cooling procedure of the SQUID is a critical point to reduce the noise when measuring later. Some advantages in comparison to the traditional low temperature-conducting SQUIDs have been pointed out. In addition a characterization of a batch of HTS SQUIDs has been done. Some suggestions about future work are also described.

The future research in this project looks promising: The development of new and cheap MEG MRI systems that will be used as a safe tool to study how the brain works.

8. References

[1] John Clarke and Alex I. Braginski. *The SQUID Handbook*, volume I. Fundamentals and technology of SQUIDs and SQUID systems. WILEY-VCH Verlag GmbH & Co. KGaA. Weinheim 2004.

[2] John Clarke and Alex I. Braginski. *The SQUID Handbook*, volume II. Applications of SQUIDs and SQUID Systems. WILEY-VCH Verlag GmbH & Co. KGaA. Weinheim 2006.

[3] Cooper, Bardeen, Schrieffer. Theory of Superconductivity.108, Phys. Rev. (1957)

[4] Fredrik Oisjoen. Licenciate thesis. Development of High-Tc SQUIDS Gradiometers. Department of microtechnology and nanoscience, CHALMERS UNIVERSITY OF TECHNOLOGY.

[5] Frederico A.C. Azevedo et al. Equal numbers of neuronal and nonneuronal cells make the human brain an isometrically scaled-up primate brain. The Journal of Comparative Neurology. Volume 513 Issue 5, Pages 532 - 541

[6] Bente Pakkenberga et al. “Aging and the human neocortex”. Elsevier, Experimental Gerontollogy 38 (2003) 95–99.

[7] Per Magnelind. Phd Thesis. “Neurons and SQUIDs, development of a system for measurements of magnetic fields generated by neurons”. Department of microtechnology and nanoscience, CHALMERS UNIVERSITY OF TECHNOLOGY. (2003)

[8] Andrä, Wilfried / Nowak, Hannes (eds.) “Magnetism in Medicine A Handbook”. Wiley-VCH, Berlin. (2007)

[9] Kirschfeld, K. “The modulation of alpha-wave amplitude in human EEG by the intention to act with a motor response”. Max-Planck-Institut für biologische Kybernetik, Spemannstr. 38, 72076 Tübingen, Germany. (2009)

[10] Vrba , J. Robinson, S. “Signal Processing in Magnetoencephalography”. METHODS **25,** 249–271 (2001)

[11] Wikswo, J. P., Jr. (1989) *in* Advances in Biomagnetism. Plenum, pp.1–18, New York/London

[12] The MEG system, UUMSI at the University of Utah. Available http://uuhsc.utah.edu/uumsi/ourmegsystem.html . Last accesed May 15th 2010

[13] Hämäläinen, M. *Magnetoencephalography – theory, instrumentation, and applications to noninvasive studies of the working human brain*. Low Temperature Laboratory, Helsinki University of Technology, 02150, Finland. Rev. Mod. Phys, Vol 65. No.2 2, April 1993

[14] H. Ohta *et al*. “Neuromagnetic squid measurements in a helmet-type superconductingmagnetic shield of bscco”:

[15] Bong-Soo Kim *et al.* “Discrimination of Multiple Sources of Alpha Brain Activity With 3-D MEG Measurement”. IEEE TRANSACTIONS ON MAGNETICS, VOL. 38, NO. 5, SEPTEMBER 2002

[16] Romani, Gian Luca. “Biomagnetism: an application of squid sensors to medicine and physiology”. Istituto di Elettronica dello Stato Solid, Roma, Physica B+C, Volume 126, Issues 1-3, November 1984.

[17] Wikswo, John P. “SQUID magnetometers for biomagnetism and non-destructive testing: important questions and initial answers”. IEEE Transactions on Applied Superconductivity 5: 74–120. (1995).

[18] Mikael Elam, MD at Neurophysiology Section of Sahlgrenska University Hospital. (2010)

[19] Konn Daniel. “Initial attempts at directly detecting alpha wave activity in the brain using MRI”. Magnetic Resonance Imaging 22 (2004) 1413–1427

[20] Tarte et al. “High Tc SQUID systems for magnetophysiology”. Physica C 368 (2002) 50–54

[21] Y. Zhang et al. “Magnetoencephalography Using High T_c SQUIDs”. Brain Topography, Volume 5, Number 4 (1993)

[22] M. S. DiIorio et al. “Biomagnetic measurements using low-noise integrated SQUID magnetometers operating in liquid nitrogen”. Biomagnetic Technologies, Inc., San Diego, California (1995)

Appendix 1: MATLAB codes of simulation

```
%%%NEAR SOURCE

%The permeability of vacuum In Henrys per Metre, the intensity in
Amperes,
%the length of the dendrite in metres and the density of neurons x
unit of
%m^2 (from Brain Research Bulletin)

clear all

%Define constants
mu0 = 4*pi*10^(-7); %[m∑Kg/(s^2∑a^2)]
m=1e-9; %Magnitude of the dipole moment for a surface activation of
40 mm^2, [Amperes∑m^2], (Hamalainen paper)

iterations = 100;

y = linspace(0,0.01,iterations);
z = linspace(0,0.01,iterations);
dy = diff(y(1:2));
dz = diff(z(1:2));

%Discretize the space(create mesh)
[y1,z1] = ndgrid(y,z);

%Magnetic field created by neurons assuming that the neurons are
uniformily
%ditributed throughout a plane perpendicular to the detector plane:
xmax = 0.14;
xmin = xmax/iterations;
x = (xmin:(xmax-xmin)/(iterations-1):xmax);
size(x)

Bb=zeros(iterations,1);
Bx=zeros(iterations,iterations);

for n = 1:iterations


    %%Only consider Bx ibecause of the dipole configuration


Bx=((mu0*3*m)/(4*pi)).*((x(n).^2)./((x(n).^2+y1.^2+z1.^2).^2.5)+1./
(x(n).^2+y1.^2+z1.^2).^1.5);
```

```
%By=((mu0*3*m)/(4*pi)).*(x(n).*y1)./((x(n).^2+y1.^2+z1.^2).^2.5);

%Bz=((mu0*3*m)/(4*pi)).*(x(n).*z1)./((x(n).^2+y1.^2+z1.^2).^2.5);
    %B=abs((Bx.^2+By.^2+Bz.^2)^0.5);

    Bb(n) = sum(sum(Bx))*dy*dz*4;
%     pause;


end
% Bb(iterations)

%Sense of numbers: Flux created by dipole at the gradiometer 1 cm
Rg=10e-4;

F10=Bb(floor(iterations*0.01/xmax))*pi*Rg^2
%Sense of numbers: Flux created by dipole at the gradiometer 2 cm
F20=Bb(floor(iterations*.02/xmax))*pi*Rg^2
%Sense of numbers: Flux created by dipole at the gradiometer 3 cm
F30=Bb(floor(iterations*.03/xmax))*pi*Rg^2
%Sense of numbers: Flux created by dipole at the gradiometer 4 cm
F40=Bb(floor(iterations*.04/xmax))*pi*Rg^2

F11=Bb(floor(iterations*.11/xmax))*pi*Rg^2
%Sense of numbers: Flux created by dipole at the gradiometer 2 cm
F12=Bb(floor(iterations*.12/xmax))*pi*Rg^2
%Sense of numbers: Flux created by dipole at the gradiometer 3 cm
F13=Bb(floor(iterations*.13/xmax))*pi*Rg^2
%Sense of numbers: Flux created by dipole at the gradiometer 4 cm
F14=Bb(floor(iterations*.14/xmax))*pi*Rg^2
%Ratios

F10/F20
F10/F30
F10/F40



F11/F12
F11/F13
F11/F14

figure (1)
semilogy(x,Bb,'r');
grid on;

axis tight;
xlabel('Distance from the source (m)')
ylabel('Magnetic field (T)')

figure(2);
% length(x(1:floor(iterations*0.12/xmax)))
```

```
% length(Bb(1:floor(iterations*0.12/xmax)))
% length(Bb(ceil(iterations*0.02/xmax):iterations-1))
meas_spacing = [0.01,0.02,0.03,0.04];
plot(x(1:floor(iterations*(xmax-meas_spacing(1))/xmax)), ...
    Bb(1:floor(iterations*(xmax-
meas_spacing(1))/xmax))./Bb(ceil(iterations*meas_spacing(1)/xmax):i
terations-1), ...
    x(1:floor(iterations*(xmax-meas_spacing(2))/xmax)), ...
    Bb(1:floor(iterations*(xmax-
meas_spacing(2))/xmax))./Bb(ceil(iterations*meas_spacing(2)/xmax):i
terations-1), ...
    x(1:floor(iterations*(xmax-meas_spacing(3))/xmax)), ...
    Bb(1:floor(iterations*(xmax-
meas_spacing(3))/xmax))./Bb(ceil(iterations*meas_spacing(3)/xmax):i
terations-1), ...
    x(1:floor(iterations*(xmax-meas_spacing(4))/xmax)), ...
    Bb(1:floor(iterations*(xmax-
meas_spacing(4))/xmax))./Bb(ceil(iterations*meas_spacing(4)/xmax):i
terations-1));

hold off;
grid on;
axis([0.01,.1,0,50]);
xlabel('Source Depth (m)');
ylabel('Signal Ratio');
legend('1 cm Low-Tc Standoff','2 cm Low-Tc Standoff','3 cm Low-Tc
Standoff','4 cm Low-Tc Standoff');

title('Hight-T_C Signal Advantage at 0 cm Standoff')
```